BIOTECHNOLOGY
and
BIOENGINEERING

Quantitative Characterization of Virus-like Particles by Asymmetrical Flow Field Flow Fractionation, Electrospray Differential Mobility Analysis, and Transmission Electron Microscopy

Leonard F. Pease III,[1*] Daniel I. Lipin,[2*] De-Hao Tsai,[1,3] Michael R. Zachariah,[1,3] Linda H.L. Lua,[2] Michael J. Tarlov,[1] Anton P.J. Middelberg[2]

[1]National Institute of Standards and Technology (NIST), Gaithersburg, Maryland

[2]Centre for Biomolecular Engineering, Australian Institute for Bioengineering and Nanotechnology, The University of Queensland, St Lucia, Brisbane 4072, Australia; telephone: +61-7-3346-4189; fax: +61-7-3346-4197; e-mail: cbe@uq.edu.au

[3]The University of Maryland, College Park, Maryland

ABSTRACT: Here we characterize virus-like particles (VLPs) by three very distinct, orthogonal, and quantitative techniques: electrospray differential mobility analysis (ES-DMA), asymmetric flow field-flow fractionation with multi-angle light scattering detection (AFFFF-MALS) and transmission electron microscopy (TEM). VLPs are biomolecular particles assembled from viral proteins with applications ranging from synthetic vaccines to vectors for delivery of gene and drug therapies. VLPs may have polydispersed, multimodal size distributions, where the size distribution can be altered by subtle changes in the production process. These three techniques detect subtle size differences in VLPs derived from the non-enveloped murine polyomavirus (MPV) following: (i) functionalization of the surface of VLPs with an influenza viral peptide fragment; (ii) packaging of foreign protein internally within the VLPs; and (iii) packaging of genomic DNA internally within the VLPs. These results demonstrate that ES-DMA and AFFFF-MALS are able to quantitatively determine VLP size distributions with greater rapidity and statistical significance than TEM, providing useful technologies for product development and process analytics.

Biotechnol. Bioeng. 2009;102: 845–855.

© 2008 Wiley Periodicals, Inc.

Introduction

Virus-like particles (VLPs) are an important class of biomolecular particles composed of self-assembling viral proteins (Pattenden et al., 2005). VLPs hold potential for a variety of applications from synthetic vaccines to protective vectors for delivery of gene and drug therapies (Garcea and Gissmann, 2004; Noad and Roy, 2003). VLP-vaccines for strains of human papillomavirus (HPV) (Koutsky et al., 2002) and Hepatitis B virus (Scolnick et al., 1984) have already received regulatory approval, and more VLP-vaccines are traversing the pipeline for viruses such as H5N1 influenza (Pushko et al., 2005). However, to ensure the safety of the public while decreasing the cost of these products, advanced measurement methods are necessary to confirm the size, integrity, stability, and aggregation state of the VLPs. Such tools are the focus of this article and have a key role in underpinning FDA initiatives directed at encouraging the development of new process analytical technologies (DePalma, 2004; FDA, 2004).

Our study centers on VLPs derived from the non-enveloped virus family polyomaviridae. The capsid shell of the murine polyomavirus (MPV) contains 72 pentamers ($T = 7d$ symmetry) of the major structural protein VP1

(Rayment et al., 1982), with minor structural proteins, VP2, and VP3, bound to the inner core of each pentamer (Barouch and Harrison, 1994). Ideally, the pentamers assemble into a shell with regular icosahedral geometry. VLP assembly in the absence of the minor structural proteins is possible (Salunke et al., 1986).

VLPs may be modified with protein sequences either displayed externally on the VLP surface (Gedvilaite et al., 2000) or else encapsulated internally within the VLP (Boura et al., 2005). VLPs may also encapsulate non-viral DNA for transfer into a cell (Forstova et al., 1995). Analytical methods are required to confirm experimentally how such modifications affect VLP size and integrity. Existing methods include transmission electron microscopy (TEM) (Boura et al., 2005; Gedvilaite et al., 2000; Gillock et al., 1997), cryogenic TEM (Charpilienne et al., 2001; Hagensee et al., 1994), size exclusion chromatography (Schmidt et al., 2001), dynamic light scattering (DLS) (Tsoka et al., 1999), analytical ultra-centrifugation (AUC) (Gleiter et al., 1999; Gleiter and Lilie, 2003), and atomic/scanning force microscopy (Yamada et al., 2003). These methods can be insensitive to subtle changes in VLP structure, subject to intensive and laborious image analysis, or else require extensive time for sample preparation or protocol development to obtain reliable results. Procedural complexity also creates the possibility of operator bias. Here we examine two emerging techniques that can provide rapid, accurate, and statistically significant size distributions for VLPs in solution. We compare electrospray differential mobility analysis (ES-DMA) and asymmetric flow field-flow fractionation using multi-angle light scattering detection (AFFFF-MALS) with TEM, contrasting and cross comparing their results for both modified and unmodified VLPs.

AFFFF-MALS is a technique that separates hydrated particles based on their size (Shortt et al., 1996). Figure 1a provides a schematic representation of AFFFF. Operation proceeds in three serial steps. In the first step (Inject + Focus), particles are injected into a 350 μm high separation channel with a porous membrane along the bottom surface of the channel. Fluid enters the channel from both ends and elutes through the porous membrane, focusing particles along the width of the channel entrance. In the second step (Elution + Cross-flow), the flow pattern is adjusted to achieve laminar flow across the channel while still maintaining cross-flow through the membrane. Particles diffuse from the membrane surface into the laminar channel flow at a rate dependent on size, allowing for small particles to elute before larger particles. The final step (Elution − Cross-flow) ceases flow through the membrane, causing all remaining large particles (and aggregates) to exit the channel. Serial analysis of eluant using UV absorbance and MALS detectors allows for determination of VLP size using the Zimm Fit Method (Zimm, 1948) (Fig. 1b). The strong UV signal in this figure highlights the resolution of the size reading for the VLP peak (root mean squared (r.m.s.) radius of gyration = 21.5 ± 0.7 nm). A typical run takes 1 h, and careful control of channel-flow and
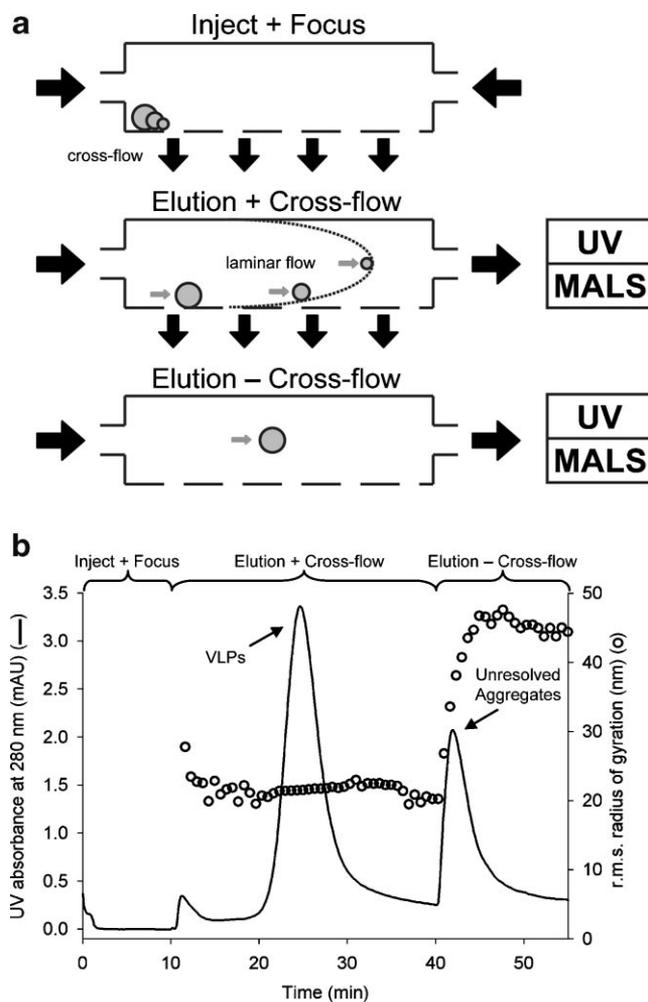
Figure 1. **a**: Separation mechanism of asymmetric field flow fractionation (AFFFF). **b**: Representative AFFFF-MALS fractogram for MPV VLPs lacking packaged genomic DNA, (sampled prior to dialysis against 20 mmol/L ammonium acetate, pH 6.7). UV absorbance and MALS detectors were used to determine the r.m.s. radius of gyration of particles eluting from the AFFFF channel.

cross-flow minimizes or eliminates possible aggregation from sample-to-sample and sample-membrane interactions (Chuan et al., 2008). AFFFF-MALS has only recently been used to analyse VLPs, although it has been used to size viruses including influenza (Wei et al., 2007) and polystyrene nanoparticles of similar size with a precision of ±1 nm (Shortt et al., 1996).

ES-DMA (Fig. 2) sizes dry particles based on their electrical mobility, similar to capillary electrophoresis (Pease et al., 2007). In the first step of a continuous process, particle solutions are electrosprayed to produce highly charged droplets. These droplets then pass into a charge neutralization chamber, which dries the droplets and fixes the charge on the particle (Bacher et al., 2001). For example, neutralization of 45 nm particles yields a charge distribution consisting of 61.5% with a net neutral charge, 16.1% with a single positive charge, 0.5% with a double positive charge,
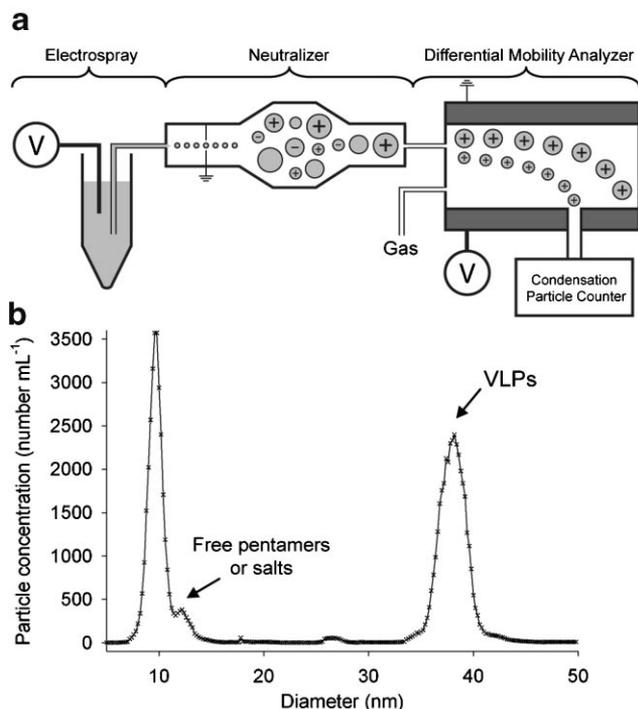
Figure 2. **a**: Major components of the ES-DMA analysis system: electrospray (ES) to convey the particles from liquid to gas phase, a neutralizer to give a majority of positively charged particles analyzed a single charge, a differential mobility analyzer (DMA) to separate and collect particles based on a trajectory determined by their electrical-to-drag force ratio, and a CPC to enumerate the particles. **b**: Representative ES-DMA size distribution plotting gas phase particle concentration versus mobility diameter for MPV VLPs lacking packaged genomic DNA (sampled after dialysis against 20 mmol/L ammonium acetate, pH 6.7). Key features include free pentamers and salts (<20 nm) as well as individual VLPs (>20 nm).

21.1% with a single negative charge, 0.8% with a double negative charge, and only 0.01% with charges outside this range (Wiedensohler, 1988). Upon entry into the DMA, only positively charged particles are deflected toward the collection slit. These particles are separated based on their electrical mobility. Like electrophoretic mobility of capillary electrophoresis, electrical mobility is proportional to the charge of the particle and inversely proportional to particle size. Because a vast majority of positively charged particles possess a +1 charge (>95% of 45 nm particles), essentially only particles of a particular size will traverse the collection slit into a condensation particle counter (CPC). Within the CPC, particles pass through a saturated butanol vapor and grow into droplets several microns in size, which can then be counted individually as they obscure light impinging on a photodetector. The total number of particles passing through the detector is then summed and reported (Fig. 2b). While ES-DMA does not differentiate between rigid spheres that are hollow or filled, it can accurately detect particles as small as 3 nm with a resolution that allows for the detection of sub-nanometer shifts in particle size (Tsai et al., 2008).

ES-DMA has been used to analyze viruses, including MS2, T2, T4, λ-phage (Hogan et al., 2005, 2006), rhinovirus (Bacher et al., 2001), rice yellow mottle virus (RYMV), and adenovirus (Thomas et al., 2004). We have also recently characterized bacteriophages pp7, φX174, and PR772 (Lute et al., 2008). ES-DMA has yet, to our knowledge, to be used to characterize modified or unmodified VLPs. A key result of previous studies has been the finding that spherical viruses can retain their viability after electrospraying. For example, Hogan et al. (2006) and Siuzdak et al. (1996) showed that the bacteriophages MS2, the RYMV, and the tobacco mosaic virus were all viable and intact after being subjected to the electrospray process. We have also recently shown that aggregates of antibodies survive the electrospray process (Pease et al., 2008). These aggregates were weakly associated dimers and trimers that were not chemically bonded. Thus, VLPs that have survived repeated freeze–thaw cycles such as those we consider herein can be expected to survive the electrospray process reasonably well.

The remainder of this study describes ES-DMA, AFFFF-MALS, and TEM sample preparation and instrument operating conditions. These techniques were used to characterize both modified and unmodified VLPs. Specifically, we examined VLPs encapsulating either genomic DNA or non-viral DNA, VLPs with outer surfaces modified to expose foreign peptide sequences, and VLPs with an internal foreign protein. We then conclude with a brief comparison of the methods.

Materials and Methods

Baculovirus Preparation

The recombinant baculovirus for expression of MPV VP1 (GenBank accession number: M34958) in insect cells was prepared as described by Chuan et al. (2008). The pENTR-VP1 plasmid utilized in preparation of this baculovirus was further modified to insert a 17 residue segment of the HA protein of avian influenza (A/Vietnam/3028/2004) into one of the surface loops (SL) of the VP1 protein (Supplementary Fig. 2). pENTR-VP1-SL was created by subjecting pENTR-VP1 to site directed mutagenesis (QuikChange II Kit, Stratagene, La Jolla, CA) to replace VP1-D86 with GCCGGC, the sequence for the blunt-end cloning enzyme *Nae*I (Primers: 5′-GATTAATTTGGCTACATCAGCCGG-CACAGAGGATTCCCC-3′, 5′-GGGGAATCCTCTGTGC-CGGCTGATGTA-GCCAAATTAATC-3′). Oligos for the HA protein segment were then inserted into pENTR-VP1-SL using *Nae*I according to the manufacturer's protocol (New England Biolabs, Beverly, MA) to create pENTR-VP1-HA (Oligos: 5′-CCGAAC-GATGCGGCGGAACAGACCA-AACTGTATCAGAACCC-GACCACCTAT-3′, 5′-ATAGG-TGGTCGGGTTCTGATACAGTTTGGTCTGTTCCGCCG-CATCGTTCGG-3′). Foreign protein (FP) encapsulation was achieved by co-expression of VP2 (GenBank accession number: AF442959) with a series of glutathione-S-transferase,

S and His tags fused to its N-terminus; the resulting capsid proteins were labeled VP2-FP. VP2-FP was prepared by cloning the VP2 sequence into pET-41a(+) (Merck Biosciences Kilsyth, VIC, Australia) between the *Eco*RI and *Sal*I points of its multiple cloning region (Primers: 5′-CCGGAATTCATGGGAGCCGCACTGACTATTCTA-3′, 5′-ACCGGTCGACTTAGAGACGCCGCTT-TTTCTTTTG-3′). Insect cell co-expression of VP1 and VP2-FP was achieved using the pFast-Bac-Dual vector (Invitrogen Corporation, Carlsbad, CA). pFast-Bac-VP1: VP2-FP was created by inserting the VP1 sequence downstream of the PH promoter site between the *Eco*RI and *Sal*I restriction sites (Primers: 5′-ACCGGAA-TTCATGGCCCCCAAAAG-AAAAAGC-3′; 5′-GGTGGTGT-CGACTTAATTTCCAGG-AAATACAGTC-3′) and inserting the VP2-FP sequence downstream of the P10 promoter site between the *Xho*I and *Sph*I restriction sites (Primers: 5′-CCG CTC GAG ATGA-TACTAGGTTATTGGAAAATTAAG-3′; 5′-GGTGGTGTC-GACTTAATTTCCAGGAAAT-ACAGTC-3′). The protein sequences derived from plasmid vectors were validated by sequencing analysis (AGRF, Brisbane, QLD, Australia). The recombinant *Autographa californica* multiple nucleopolyhedroviruses (AcMNPV) for expression of VP1 or VP1-HA were generated from pENTR-VP1 and pENTR-VP1-HA respectively using the BaculoDirect™ baculovirus expression system (Invitrogen) as described by the manufacturer. Recombinant AcMNPV for co-expression of VP1 and VP2-FP were generated from pFast-Bac-VP1:VP2-FP using the Bac-to-Bac®, baculovirus expression system (Invitrogen) as described by the manufacturer.

Expression and Purification

The protocol for expression and purification of each VLP type was similar to that from Chuan et al. (2008). Protein was expressed using Sf9 insect cells, with a cell density at time of infection of 3×10^6 cells mL^{-1} and a multiplicity of infection of five plaque forming units (PFU) mL^{-1}. At 72 h post-infection, cells were harvested and re-suspended in Lysis Buffer (50 mmol/L MOPS, 500 mmol/L NaCl, 0.01% Tween 80, pH 7.0). Cell suspensions were subjected to three cycles of sonication (45 s at 55 W) and then centrifuged to remove insoluble material. Supernatants were layered on 30% (v/v) sucrose in Lysis Buffer and centrifuged for 90 min at 175,000 g, 4°C. Pellets were re-suspended in Lysis Buffer, sonicated briefly at low power, and centrifuged to remove insoluble material. Supernatants were mixed with cesium chloride up to a density of 1.26 $g\,L^{-1}$ and centrifuged at 337,000 g, 4°C for 16 h. Observable bands of protein were extracted from the top of each centrifugation tube by needle syringe. VP1 and VP1-HA expression yielded centrifugation tubes with two bands. It was assumed based on previous studies that the top bands contained VLPs without packaged genomic DNA, while bottom bands contained VLPs with packaged genomic DNA (Gillock et al., 1997). For VP1 expression, both top and bottom bands were extracted. For VP1-HA expression, the top band yielded negligible

quantities of protein and so only the bottom band was extracted. Co-expression of VP1 & VP2-FP yielded a single band, which has been shown to contain VLPs without packaged genomic DNA (data not shown). Extracted band solutions were dialyzed against 20 mmol/L ammonium acetate, pH 6.7 at 4°C, changing the buffer three times over 5 h. Dialysis cartridges used 10 kDa Snakeskin dialysis tubing (Pierce Biotechnology, Rockford, IL). Dialyzed solutions were centrifuged to remove insoluble material. Each of these solutions had conductivities <0.2 S m^{-1} as determined using an AKTÄ™ Explorer Conductivity Meter (GE Healthcare, Uppsala, Sweden). Protein concentrations for all solutions were determined using a Bioanalyzer™ P230 protein analysis system (Supplementary Table S1) (Agilent Technologies, Santa Clara, CA). Solutions were stored at 4°C.

Size Distribution Analysis

Prior to the dialysis stage of the purification protocol, solutions were analyzed with AFFFF-MALS and TEM. After the dialysis stage was completed, solutions were then partitioned into two sets. The first set was shipped from The University of Queensland (UQ) to NIST at 4°C and was analyzed by ES-DMA 4 days later. The second set was retained at UQ at 4°C for the same period of time, for subsequent analysis by AFFFF-MALS.

Transmission Electron Microscopy

Samples were coated onto glow-discharged carbon-coated grids at room temperature for 2 min. Grids were then washed with deionized water, stained with 2% (w/v) uranyl acetate and examined using a JEOL 1011 microscope. All images were captured by a Soft Imaging Megaview III (Olympus Soft Imaging Solutions Corp., Lakewood, CO) at 200,000× magnification. Images were printed and a representative diameter was selected for each non-overlapping particle. Where the particle was ellipsoidal in shape a representative diameter between those of the major and minor axis was selected. Image analysis was performed with at Westcott Ruler (Acme United Corporation, Fairfield, CT) marked every 1 mm with each millimeter corresponding to 2.4 nm. At least 200 counts were used to prepare each histogram, binned every 2.5 nm to reflect uncertainty in the measurement implement. Averages reported are simple averages over all diameters collected for the sample. Photoshop software (Adobe Systems Incorporated, San Jose, CA) was used to adjust the brightness and contrast of each image.

Asymmetrical Flow Field-flow Fractionation With Multiple Angle Light Scattering

AFFFF-MALS analysis was conducted using the Eclipse 2 AFFFF system (Wyatt Technology Corporation, Santa Barbara, CA) together with Agilent 1100 Series equipment

(Agilent Technologies) as described by Chuan et al. (2008). All operations were conducted using AFFFF Buffer (10 mmol/L Tris, 50 mmol/L NaCl, 0.01 mmol/L CaCl$_2$, pH 8.0). For each analysis run, the AFFFF system was maintained in Inject + Focus mode for the first 10 min (Fig. 1A), with buffer passed into the channel from both the inlet and outlet points at a flow ratio of 1:9. Samples were injected (undiluted) into the channel during this time. From 10 to 40 min the system was switched to Elution + Cross-flow mode, with flow through the channel set to 0.75 mL min^{-1} and cross-flow through the membrane set to 0.75 mL min^{-1}. From 40 min on cross-flow was ceased until all remaining particles were eluted from the channel. Eluant was passed through a sequence of UV absorbance and MALS detectors for size analysis. The r.m.s. radius of gyration of eluted species was determined using Astra V software's Zimm Fit Function (Wyatt Technology Corporation), described in detail in Wyatt (1993). For the purposes of this study, the UV extinction coefficient for all protein ($\varepsilon_{0.1\%}$) was assumed to be 1.36 mL mg^{-1} cm^{-1} (theoretical value calculated from amino acid sequence of VP1) (Gasteiger et al., 2005) and the differential refractive index (dn/dc) for all protein was assumed to be constant at 0.185 mL g^{-1} (Huglin, 1972). The concentrations of VLPs used in this study were low enough for small variations in either $\varepsilon_{0.1\%}$ or dn/dc to have negligible effects on r.m.s. radius of gyration calculations. To improve the comparability of data across instruments we rebinned the AFFFF-MALS data into bins spanning 0.2 nm with the help of an Excel Macro. Particles in the 18.0 nm bin, for example, range in size from 17.9 to 18.1 nm.

Electrospray Differential Mobility Analysis

Solutions were electrosprayed with an Electrospray Aerosol Generator (TSI Inc., Shoreview, MN, #3480) through a nominally 25 μm inner diameter capillary with a tapered outlet (Fig. 2A). The stable cone-jet condition necessary to obtain reliable results was achieved by maintaining potentials from approximately 1.96 to 2.22 kV and using gas flow rates of 0.2 L min^{-1} of CO$_2$ and 1.0 L min^{-1} of air. Droplet evaporation left dry particles, which transited the approximately 1.4 m of plastic Tygon tubing (1.6 cm diameter) connecting the exit of the ES to the entrance of the DMA. Charge neutralizers rebalanced the charge distribution at both the exit and the entrance of the tubing to achieve a modified Boltzmann distribution (Wiedensohler, 1988). Flow containing dry particles joined a flow of nitrogen gas at 30 L min^{-1} in an annular analysis chamber (TSI Inc., #3080), with an electrostatic potential as strong as −10 kV deflecting positively charged particles toward a collection slit and then into the CPC (TSI Inc., #3025A). The 1.0 L min^{-1} flow exiting the DMA was supplemented by 0.5 L min^{-1} of ambient air filtered through a HEPA filter. Within the CPC, particles pass through a saturated butanol environment and grow into droplets several microns in size, which can be counted individually as they obscure light

impinging on a photodetector. Particles 3 nm to 50 nm in diameter were collected in 0.2 nm increments, with CPC analysis of each size conducted for 20 s.

Conversion to size was performed assuming the particles to be spheres with a Cunningham slip correction factor of $C_c = 1 + Kn[\alpha + \beta \exp(-\gamma/Kn)]$, where $Kn = 2\lambda/d$, d is the particle's diameter, $\alpha = 1.257$, $\beta = 0.40$, $\gamma = 1.110$, and the gas mean free path at room temperature $\lambda = 66$ nm (Pease et al., 2007). The mean or number–average diameter was then calculated with $\overline{d} = \sum_i d_i N_i / \sum_i N_i$, where N_i is the number of particles counted by the CPC of size d_i.

Results and Discussion

In this section we report our characterization of VLPs by ES-DMA, AFFFF-MALS, and TEM. The four samples used in this study are depicted in Figure 3. First, we examine the difference in the size between VLPs with and without packaged DNA (Fig. 3a and c). We then modify a surface loop of the VP1 pentamer with a foreign peptide sequence from the influenza virus HA protein to determine whether AFFFF-MALS and ES-DMA can detect a size shift following the chimeric modification of the VLP surface (Fig. 3c and d). We also determine whether VP2-directed packaging of protein into VLPs causes a size shift that can be detected
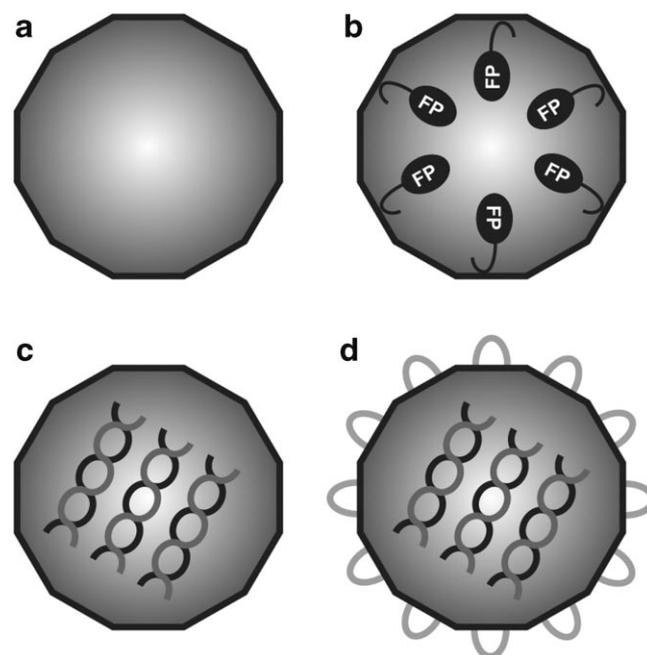
Figure 3. MPV VLP types analyzed in this study (**a**) VLP without packaged genomic DNA or protein (VLP w/o DNA). **b**: VLP with packaged FP (VLP + VP2-FP). **c**: VLP with packaged genomic DNA (VLP + DNA). **d**: VLP assembled from VP1 pentamers modified to express a foreign peptide sequence on the VLP surface (VP1-HA), while also containing packaged genomic DNA (VLP-HA + DNA).

with these methods (Fig. 3a and b). Finally, we conclude with a brief comparison of the methods.

TEM analysis highlights how the inherent icosahedral geometry of VLPs and their crystal structure alone do not conclusively determine their size or shape (Fig. 4). Although capsid proteins in polyomavirus are known to retain an icosahedral surface lattice, TEM shows the VLPs in this study to be primarily spherical in shape (Finch, 1974). Close inspection of TEM micrographs further indicates that some particles more closely resemble ellipsoids than spheres. This is particularly true of "empty" VLPs (upper left) where the major axis of the ellipsoid can be 40% longer than the minor axis. TEM analyses of "empty" VLPs in the literature have also yielded images of particles that are less spherical and more prone to "squashing" (Gillock et al., 1997; Gleiter et al., 1999; Pawlita et al., 1996). It is probable that this deformation of VLPs is due to the absence of virus specific nucleic acids and histones from the capsid interior, which may provide structural support against substrate–virus attraction (i.e., van der Waals forces). Deformation of VLPs may also occur as a consequence of their instability during fixing and staining preparation steps. Encapsulation of foreign protein also appears to cause deformations within some of the VLP structures (upper right). Similar VLP defects have been observed following the VP2-directed packaging of green fluorescent protein into MPV VLPs (Boura et al., 2005). Modification of the pentamer surface with foreign peptide sequences (lower left) has also significantly affected the integrity of the VLP structure and has made it difficult to focus on the VLP surface, which has also been previously observed (Gedvilaite et al., 2000; Ionescu et al., 2006).

While TEM provides captivating images and a sense for the particle shape, it is an expensive, and labor-intensive procedure for measuring particle size distributions. Yet, the need for rapid methods to assess the distribution of VLP sizes is particularly acute given the polydispersity in size of the VLPs in Figure 4. To meet this need, ES-DMA, and AFFFF-MALS are better suited to rapidly and cost-effectively generate statistically significant size distributions. With respect to time, ES-DMA, and AFFFF-MALS distributions for each VLP type were each completed within 1 h, whereas each TEM histogram required at least a day to compile. The sample size used by TEM analysis ($\approx$200 particles) was also far less than the $\approx 10^5$ particles analyzed by ES-DMA for each VLP type. The combination of speed and larger sample size substantially improves our ability to capture multimodal distributions and discern subtle shifts in size between VLPs, which is the focus of the remainder of this article.

Packaging of Non-Viral Nucleic Acid

Figure 5a utilizes TEM, ES-DMA, and AFFFF-MALS to compare size distributions of VLPs with and without
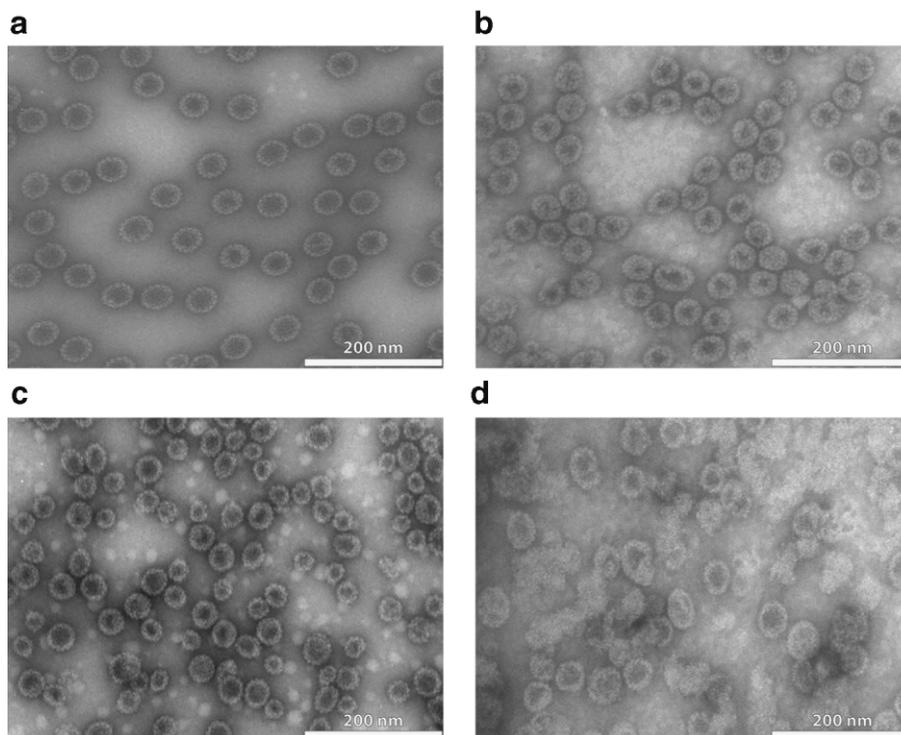
Figure 4. TEM images of VLP variants. **a**: VLP without packaged genomic DNA or protein (VLP w/o DNA). **b**: VLP with packaged FP (VLP + VP2-FP). **c**: VLP with packaged genomic DNA (VLP + DNA). **d**: VLP assembled from VP1 pentamers modified to express a foreign peptide sequence on the VLP surface (VP1-HA), while also containing packaged genomic DNA (VLP-HA + DNA).
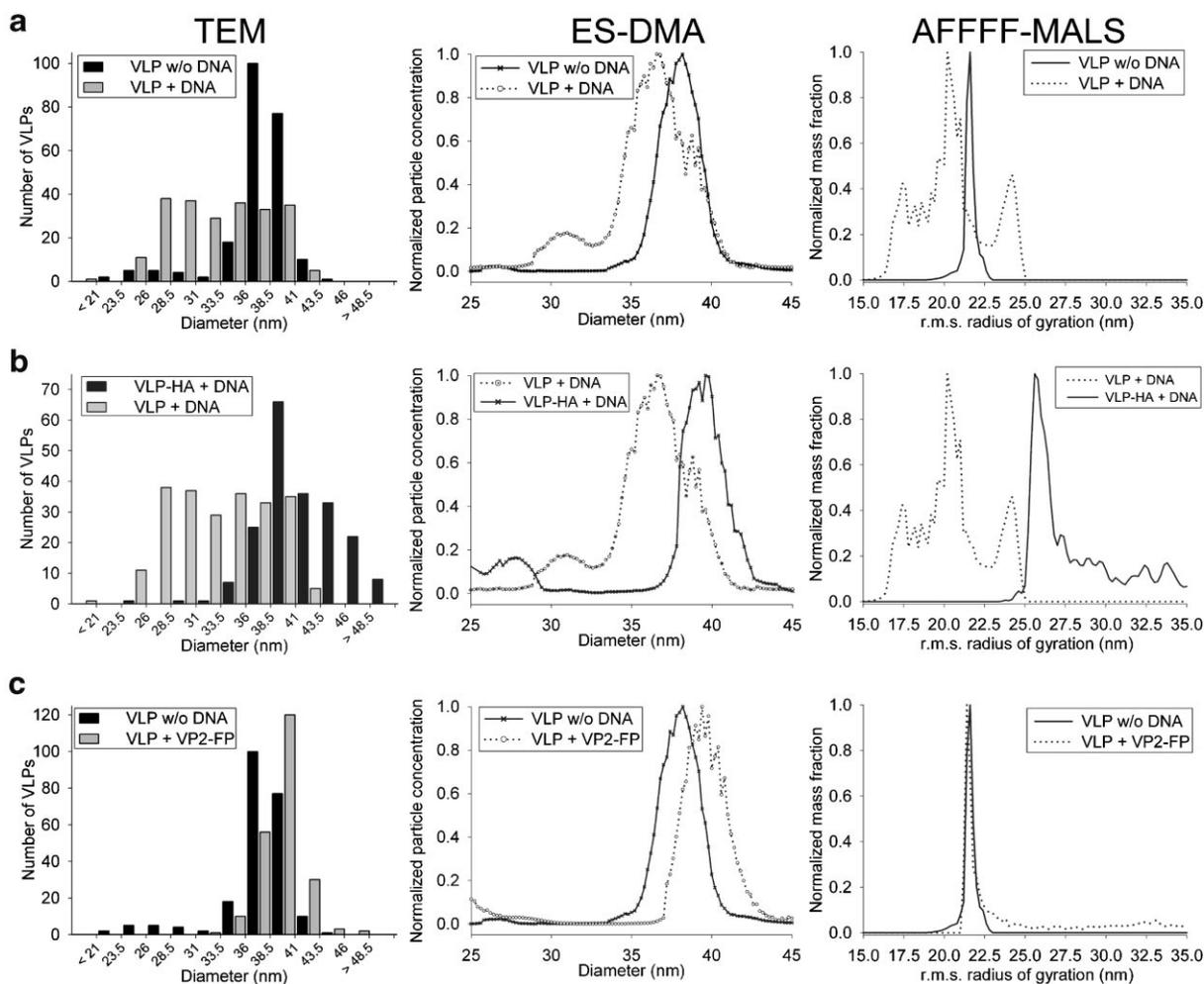
Figure 5. How modification of MPV VLPs affects their particle size distributions. VLP solutions were subjected to TEM Histogram analysis, ES-DMA analysis and AFFFF-MALS analysis to determine VLP size distributions. Comparisons: (**a**) VLPs with and without encapsulated genomic DNA. **b**: VLPs encapsulating genomic DNA with and without surface modification using a foreign peptide sequence (HA). **c**: VLPs with and without packaged FP.

packaged genomic DNA. Instruments that distinguish between these two classes of VLPs hold potential to facilitate quality control in the production of gene therapy agents. ES-DMA and AFFFF-MALS analysis both show ''empty''

VLPs (i.e., VLP w/o DNA) to be monodisperse. Table I summarize the width of the distributions (one standard deviation) for this sample to be 1.3 nm to 2.1 nm, providing an upper bound on the precision of these instruments. This

Table I. Summary of diameters and widths of distributions.

Sample	ES-DMA external diameter	AFFFF-MALS diameter of gyration		TEM external diameter
	After dialysis mean (nm)[a,b]	Before dialysis mean (nm)[b,c]	After dialysis mean (nm)[b,c]	Before dialysis mean (nm)[a]
VLP w/o DNA	38.1 ± 1.4	42.4 ± 1.3	41.4 ± 2.1	36.8 ± 3.7
VLP + DNA	35.9 ± 2.6	40.9 ± 4.5	42.2 ± 3.7	32.5 ± 4.9
VLP-HA + DNA	39.7 ± 1.3	58.3 ± 9.7	47.5 ± 5.7	42.0 ± 4.8
VLP + VP2-FP	39.6 ± 1.3	49.0 ± 9.6	47.0 ± 5.4	39.2 ± 2.7

[a]This mean represents the number-average diameter as ES-DMA and TEM report the number of particles (Hinds, 1999).
[b]Uncertainties characterize the width of the corresponding distributions assuming a monomodal normal distribution and not necessarily the repeatability or precision of the analysis instrumentation.
[cc]This mean represents the average of the mass weighted distribution of the radii of gyration and thus is a mass–average diameter (Hinds, 1999).

range is commensurate with the width of the distribution in the TEM histogram. It should be noted that at low VLP protein concentrations (Supplementary Table S1) the inherent noise that exists during AFFFF-MALS analysis had an impact on size distribution calculations.

The distribution of VLPs with packaged genomic DNA (i.e., VLP + DNA) is, in contrast, much broader and multimodal. AFFFF-MALS, ES-DMA, and TEM analysis of VLPs with packaged DNA indicate the dominant peak to be a few nanometers smaller than that for empty VLPs. It is difficult to discern from the TEM histogram whether the VLP + DNA sample's size distribution is simply broad or whether it is multimodal. In contrast, ES-DMA and AFFFF-MALS utilize a sample size large enough to indicate that the distribution is multimodal. (We note in passing that these additional shoulder peaks were not formed in the electrospray because AFFFF-MALS shows a similar multi-modal distribution.) Although the exact identity of the shoulder peaks on either side of the dominant peak cannot be confirmed from size information alone, studies based on TEM would usually be inadequate to confirm the presence of shoulder peaks in the first instance due to their lower particle counts.

One possible source of the multimodal distribution may be the in vivo assembly process. The breaking down of insect cell genomic DNA into approximately 5 kbp strands for packaging into MPV VLPs is a process that takes 5 days (post-infection) to complete (Gillock et al., 1997). At 3 days post-infection (when the cells were harvested), MPV VLPs can encapsulate lower molecular weight DNA strands in addition to the 5 kbp DNA strands (Gillock et al., 1997). Packaging different nucleic acid lengths can affect the size of the VLP. For example, Tsukamoto et al. (2007) showed that packaging lower molecular weight linear DNA in VLPs caused significant decreases in size. Similarly, studies of the packaging of RNA strands of varied length (Thomas et al., 2004) of the cowpea mosaic virus with ES-DMA found that encapsulation of longer RNA strands increased the average diameter of the virus by approximately 1 nm. Nevertheless, this is the first report in the literature of ES-DMA distinguishing VLPs with and without encapsulated non-viral DNA.

Why encapsulation of genomic DNA causes the dominant VLP species to be slightly smaller than "empty" VLPs may be due to the electrostatic attraction between the N-terminus of VP1 and DNA (Moreland et al., 1991). It is possible that packaged DNA pulls on the N-termini of the VP1 pentamers, causing them to compact closer together, which would decrease the overall size of the VLP. Compression of VLP structural proteins following the encapsulation of DNA has been theorized previously in agreement with our observations (Fligge et al., 2001; Schafer et al., 2002; Voronkova et al., 2007).

Rapid means of detecting the proportion of VLPs containing nucleic acids is a valuable attribute of AFFFF-MALS and ES-DMA with important applications. For example, conventional production processes (e.g., for recombinant adeno-associated viruses) yield large quantities of non-infectious particles that are likely to be devoid of specific DNA components (Zolotukhin et al., 1999). Techniques for rapid quantification of "full" and "empty" viruses would be invaluable for quality control of these processes. To use of VLPs as gene delivery agents (Garcea and Gissmann, 2004), methods will be required to determine the efficiency of DNA encapsulation. If regulatory approval for VLP products requires that the presence of exogenous DNA be minimized, techniques would be required for the development of processes to minimize the presence of VLPs encapsulating genomic DNA. AFFFF-MALS and ES-DMA are ideal techniques for all of these scenarios.

Surface Modification

One particularly attractive attribute of VLPs is that their surfaces can be selectively modified by recombinant techniques, an attribute of particular value to the development of innovative vaccines. ES-DMA and AFFFF-MALS can also be used to detect these modifications of the VLP surface. Figure 5b portrays the change in size upon recombinant insertion of a FP sequence, a 17 residue segment of the HA protein of avian influenza (HA), into the protein backbone of each VP1 pentamer. Upon VLP assembly, HA protrudes from the external surface of the VLP, and is expected to increase both the aerodynamic drag as well as the solution radius of gyration of the VLP. Both ES-DMA and AFFFF-MALS were able to detect an increase in the size of surface modified VLPs compared to empty VLPs. AFFFF-MALS detected an increase in diameter of 17.4 nm following the addition of HA to the VLP surface (see Table I). This increase is significant despite the several nanometer widths of the VLP-HA + DNA and VLP + DNA distributions reported in Table I. (The uncertainty of the AFFFF-MALS technique has been previously established at 1 nm to 2 nm by Shortt et al. (1996), although the low concentration of this VLP-HA sample (see Supplementary Table S1) may marginally increase the AFFFF-MALS uncertainty in this case.) This difference was confirmed by TEM analysis, which found an approximately 10 nm increase that was also statistically significant. ES-DMA also detected a 3.8 nm size difference between VLPs with and without surface modifications, which was more modest than both TEM and AFFFF-MALS measurements. A potential reason for the difference between TEM/AFFFF-MALS and ES-DMA analysis is that during the dialysis and centrifugation stage of the purification protocol, a significant quantity of HA-VLPs were lost (some of which may have been small, soluble aggregates), which could have impacted ES-DMA measurements. It is also possible that the removal of salts from HA-VLPs had a direct effect on the ability of this specific peptide sequence to protrude from the VLP surface, given that AFFFF-MALS analysis of HA-VLPs after dialysis indicated a size difference of only 5.3 nm compared with the

VLP+DNA sample (Table I). (Only HA-VLPs show a statistically significant change in size as a result of salt removal (Table I).)

Packaging of Foreign Protein

We now compare VLPs with and without encapsulated FP (see Fig. 5c), which may be used in potential applications as therapeutic delivery agents or purification tags. For our structural studies, the FP consisted of a series of glutathione-S-transferase, S and His tags, and was packaged into MPV VLPs by fusing FP to the N-terminal of VP2 (total size of VP2-FP = 67.3 kDa) (Barouch and Harrison, 1994). Determination of the protein concentration with a 2100 Bioanalyzer^{TM} yielded a VP1:VP2-FP ratio of 9:1 (see Supplementary Table S1), indicating that on average 1 VLP contains 40 copies of VP2-FP.

TEM analysis indicates an increase in diameter as a result of FP encapsulation (2.4 nm) upon comparison of the VLP + VP2-FP to the VLP w/o DNA distributions. However, this difference was also too close to the resolution of the histogram (2.5 nm) to be significant. ES-DMA indicated this increase to be 1.5 nm, but the width of the distributions (1.3 nm to 1.4 nm) combined with the uncertainty in the repeatability from run to run (0.3 nm) erase any statistical significance associated with this difference. Similarly, AFFFF-MALS finds a 6.6 nm difference, but here again the width of the VLP + VP2-FP distribution (9.6 nm) and the associated instrument precision (1 nm to 2 nm) removes our ability to assert statistical significance. Thus, while all three techniques were able to detect subtle differences in size greater than the precision of the instruments, the width of these distributions prevented these differences from being statistically distinguishing upon encapsulation of this protein. We hasten to note that this narrow conclusion would not be expected to apply for VLPs with tighter distributions like those of the VLP w/o DNA distribution.

Comparison of ES-DMA and AFFFF-MALS

In general, size measurements by ES-DMA were smaller than those of AFFFF-MALS (Table I). There are several possible reasons for this finding. First, ES-DMA is a direct measurement method so that each particle of a particular size is individually summed. The reported mean thus represents the first-moment average (Hinds, 1999). MALS, in contrast, reports an ensemble average based on the root mean square radius of gyration; a root mean square length corresponds to the second moment of a distribution. For any given distribution, the second-moment average always exceeds the first-moment (Hinds, 1999). This effect is rather modest for the distributions considered here because calculating the second moment of the distribution from the ES-DMA data contributes less than 0.1 nm to the ES-DMA mean. Also some of this rather modest effect has been

further minimized by first separating the particles with AFFFF prior to detection.

Second, ES-DMA measures the external size of the VLPs while MALS reports the radius of gyration. Directly comparing these two measures of size on a single basis involves some uncertainty because the distribution of mass within the VLP can affect the radius of gyration but not its external size. To convert the diameter of gyration into an external diameter, we multiply the former by a factor of 1.22–1.58 for solid and hollow spheres, respectively (Satterly, 1960). For example, the 42.4 nm diameter of gyration for the VLP w/o DNA corresponds to an external diameter of 51.9 nm to 67.0 nm. Thus, selection of the size metric dramatically impacts the size reported.

Third, ES-DMA involves dry measurement, while AFFFF-MALS examines particles in solution. Drying of VLPs may decrease their size and lead to a partial retraction of more hydrophilic protrusions. Comparisons of small angle neutron scattering and crystallography experiments on the bacteriophage MS2 showed a decrease in the thickness of the protein shell of 0.4 nm to 0.6 nm attributable to dehydration (Kuzmanovic et al., 2006). The effect may be more pronounced for surface proteins, like the HA protein fragments protruding from VLP surface loops considered herein, that may flap loosely in solution but collapse on the surface upon dehydration (Kuzmanovic et al., 2006). If all of the difference in external size were attributed to drying then the size of the virus would shrink by 27–43% for the VLP w/o DNA sample. Although this difference is quite substantial, it is not unreasonable. Others have found similar differences between wet and dry measurements for virus particles. For example, Lute et al. (2004) found PR772 to be 82 nm in solution by DLS while the size reported by other dry methods including TEM was 53 nm to 63 nm (for shrinkage of 23–35%). So a size difference of 40% is not unreasonable between wet and dry measurements. In any case, ES-DMA and AFFFF-MALS provide better resolution, greater statistical significance and accelerated turn around time in data collection and analysis relative to TEM.

Conclusion

In summary, we have demonstrated ES-DMA and AFFFF-MALS as valuable methods to characterize multimodal VLP distributions rapidly and quantitatively. Both instruments can detect subtle changes in size and distribution characteristic of internal packaging of nucleic acids or chimeric incorporation of surface proteins. Techniques such as ES-DMA and AFFFF-MALS will be increasingly essential as biopharmaceutical companies and regulatory agencies, such as the FDA, seek to ensure quality in the development and production of innovative vaccines and gene therapy agents based on VLPs.

References

Bacher G, Szymanski WW, Kaufman SL, Zollner P, Blaas D, Allmaier G. 2001. Charge-reduced nano electrospray ionization combined with differential mobility analysis of peptides, proteins, glycoproteins, noncovalent protein complexes and viruses. J Mass Spectrom 36(9):1038–1052.

Barouch DH, Harrison SC. 1994. Interactions among the major and minor coat proteins of polyomavirus. J Virol 68(6):3982–3989.

Boura E, Liebl D, Spisek R, Fric J, Marek M, Stokrova J, Holan V, Forstova J. 2005. Polyomavirus EGFP-pseudocapsids: Analysis of model particles for introduction of proteins and peptides into mammalian cells. FEBS Lett 579(29):6549–6558.

Charpilienne A, Nejmeddine M, Berois M, Parez N, Neumann E, Hewat E, Trugnan G, Cohen J. 2001. Individual rotavirus-like particles containing 120 molecules of fluorescent protein are visible in living cells. J Biol Chem 276(31):29361–29367.

Chuan YP, Fan YY, Lua L, Middelberg APJ. 2008. Quantitative analysis of virus-like particle size and distribution by field-flow fractionation. Biotechnol Bioeng 99(6):1425–1433.

DePalma A. 2004. PAT: Taking process monitoring to next level. Genet Eng News 24(15):46–47.

FDA. 2004. Guidance for industry: PAT—A framework for innovative pharmaceutical development, manufacturing, and quality assurance. http://www.fda.gov/cder/guidance/6419fnl.pdf.

Finch JT. 1974. Surface-structure of polyoma-virus. J Gen Virol 24:359–364.

Fligge C, Schafer F, Selinka HC, Sapp C, Sapp M. 2001. DNA-induced structural changes in the papillomavirus capsid. J Virol 75(16):7727–7731.

Forstova J, Krauzewicz N, Sandig V, Elliott J, Palkova Z, Strauss M, Griffin BE. 1995. Polyoma virus pseudocapsids as efficient carriers of heterologous DNA into mammalian cells. Hum Gene Ther 6(3):297–306.

Garcea RL, Gissmann L. 2004. Virus-like particles as vaccines and vessels for the delivery of small molecules. Curr Opin Biotechnol 15(6):513–517.

Gasteiger E, Hoogland C, Gattiker A, Duvaud S, Wilkins MR, Appel RD. 2005. In: JM W, editor. The proteomics protocols handbook. Totowa, NJ: Humana Press. p. 571–607.

Gedvilaite A, Frommel C, Sasnauskas K, Micheel B, Ozel M, Behrsing O, Staniulis J, Jandrig B, Scherneck S, Ulrich R. 2000. Formation of immunogenic virus-like particles by inserting epitopes into surface-exposed regions of hamster polyomavirus major capsid protein. Virology 273(1):21–35.

Gillock ET, Rottinghaus S, Chang D, Cai X, Smiley SA, An K, Consigli RA. 1997. Polyomavirus major capsid protein VP1 is capable of packaging cellular DNA when expressed in the baculovirus system. J Virol 71(4):2857–2865.

Gleiter S, Lilie H. 2003. Cell-type specific targeting and gene expression using a variant of polyoma VP1 virus-like particles. Biol Chem 384(2):247–255.

Gleiter S, Stubenrauch K, Lilie H. 1999. Changing the surface of a virus shell fusion of an enzyme to polyoma VP1. Protein Sci 8(12):2562–2569.

Hagensee ME, Olson NH, Baker TS, Galloway DA. 1994. 3-Dimensional structure of vaccinia virus-produced human papillomavirus type-1 capsids. J Virol 68(7):4503–4505.

Hinds WC. 1999. Aerosol technology: Properties, behavior, and measurement of airborne particles. New York: John Wiley & Sons. p. 84.

Hogan CJ, Kettleson EM, Lee MH, Ramaswami B, Angenent LT, Biswas P. 2005. Sampling methodologies and dosage assessment techniques for submicrometre and ultrafine virus aerosol particles. J Appl Microbiol 99(6):1422–1434.

Hogan CJ, Kettleson EM, Ramaswami B, Chen DR, Biswas P. 2006. Charge reduced electrospray size spectrometry of mega- and gigadalton complexes: Whole viruses and virus fragments. Anal Chem 78(3):844–852.

Huglin MB. 1972. Light scattering from polymer solutions. London, UK: Academic Press. p. 165–331.

Ionescu RM, Przysiecki CT, Liang XP, Garsky VM, Fan JA, Wang B, Troutman R, Rippeon Y, Flanagan E, Shiver J, Shi L. 2006. Pharmaceutical and immunological evaluation of human papillomavirus virus-like particle as an antigen carrier. J Pharm Sci 95(1):70–79.

Koutsky LA, Ault KA, Wheeler CM, Brown DR, Barr E, Alvarez FB, Chiacchierini LM, Jansen KU. 2002. A controlled trial of a human papillomavirus type 16 vaccine. N Engl J Med 347(21):1645–1651.

Kuzmanovic DA, Elashvili I, Wick C, O'Connell C, Krueger S. 2006. The MS2 coat protein shell is likely assembled under tension: A novel role for the MS2 bacteriophage A protein as revealed by small-angle neutron scattering. J Mol Biol 355(5):1095–1111.

Lute S, Aranha H, Tremblay D, Liang DH, Ackermann HW, Chu B, Moineau S, Brorson K. 2004. Characterization of coliphage PR772 and evaluation of its use for virus filter performance testing. Appl Environ Microbiol 70(8):4864–4871.

Lute S, Riordan W, Pease LF III, Tsai D-H, Levy R, Haque M, Martin J, Moroe I, Sato T, Morgan M, Krishnan M, Campbell J, Genest P, Dolan S, Tarrach K, Meyer A, the PDA Virus Filter Task Force, Zachariah MR, Tarlov MJ, Etzel M, Brorson KA. 2008. A consensus rating method for small virus-retentive filters. I. Method development. PDA J Pharm Sci Technol, in press.

Moreland RB, Montross L, Garcea RL. 1991. Characterization of the DNA-binding properties of the polyomavirus capsid protein-VP1. J Virol 65(3):1168–1176.

Noad R, Roy P. 2003. Virus-like particles as immunogens. Trends Microbiol 11(9):438–444.

Pattenden LK, Middelberg APJ, Niebert M, Lipin DI. 2005. Towards the preparative and large-scale precision manufacture of virus-like particles. Trends Biotechnol 23(10):523–529.

Pawlita M, Muller M, Oppenlander M, Zentgraf H, Herrmann M. 1996. DNA encapsidation by viruslike particles assembled in insect cells from the major capsid protein VP1 of B-lymphotropic papovavirus. J Virol 70(11):7517–7526.

Pease LF, Tsai D-H, Zangmeister RA, Zachariah MR, Tarlov MJ. 2007. Quantifying the surface coverage of conjugate molecules on functionalized nanoparticles. J Phys Chem C 111(46):17155–17157.

Pease LF, Elliott JT, Tsai D-H, Zachariah MR, Tarlov MJ. 2008. Determination of protein aggregation with differential mobility analysis: Application to IgG antibody. Biotechnol Bioeng 101:1214–1222.

Pushko P, Tumpey TM, Bu F, Knell J, Robinson R, Smith G. 2005. Influenza virus-like particles comprised of the HA, NA, and M1 proteins of H9N2 influenza virus induce protective immune responses in BALB/c mice. Vaccine 23(50):5751–5759.

Rayment I, Baker TS, Caspar DL, Murakami WT. 1982. Polyoma virus capsid structure at 22.5 A resolution. Nature 295(5845):110–115.

Salunke DM, Caspar DL, Garcea RL. 1986. Self-assembly of purified polyomavirus capsid protein VP1. Cell 46(6):895–904.

Satterly J. 1960. Formulae for volumnes, surface areas and radii of gyration of spheres, ellipsoids and spheroids. Math Gaz 44(347):15–19.

Schafer F, Florin L, Sapp M. 2002. DNA binding of L1 is required for human papillomavirus morphogenesis in vivo. Virology 295(1):172–181.

Schmidt U, Gunther C, Rudolph R, Bohm G. 2001. Protein and peptide delivery via engineered polyomavirus-like particles. FASEB J 15(9):1646–1648.

Scolnick EM, McLean AA, West DJ, McAleer WJ, Miller WJ, Buynak EB. 1984. Clinical-evaluation in healthy-adults of a hepatitis-B vaccine made by recombinant DNA. J Am Med Assoc 251(21):2812–2815.

Shortt DW, Roessner D, Wyatt PJ. 1996. Absolute measurement of diameter distributions of particles using a multiangle light scattering photometer coupled with flow field-flow fractionation. Am Lab 17:21.

Siuzdak G, Bothner B, Yeager M, Brugidou C, Fauquet CM, Hoey K, Chang CM. 1996. Mass spectrometry and viral analysis. Chem Biol 3(1):45–48.

Thomas JJ, Bothner B, Traina J, Benner WH, Siuzdak G. 2004. Electrospray ion mobility spectrometry of intact viruses. Spectrosc Int J 18(1):31–36.

Tsai D-H, Zangmeister RA, Pease LF, Tarlov MJ, Zachariah MR. 2008. Gas-phase ion-mobility characterization of SAM functionalized Au nano-particles. J Phys Chem C 24(16):8483–8490.

Tsoka S, Holwill I, Hoare M. 1999. Virus-like particle analysis in yeast homogenate using a laser light-scattering assay. Biotechnol Bioeng 63(3):290–297.

Tsukamoto H, Kawano M-a, Inoue T, Enomoto T, Takahashi R-u, Yokoyama N, Yamamoto N, Imai T, Kataoka K, Yamaguchi Y, et al. 2007. Evidence that SV40 VP1-DNA interactions contribute to the assembly of 40-nm spherical viral particles. Genes Cells 12(11): 1267–1279.

Voronkova T, Kazaks A, Ose V, Ozel M, Scherneck S, Pumpens P, Ulrich R. 2007. Hamster polyomavirus-derived virus-like particles are able to transfer in vitro encapsidated plasmid DNA to mammalian cells. Virus Genes 34(3):303–314.

Wei Z, McEvoy M, Razinkov V, Polozova A, Li E, Casas-Finet J, Tous GI, Balu P, Pan AA, Mehta H, et al. 2007. Biophysical characterization of influenza virus subpopulations using field flow fractionation and multiangle light scattering: Correlation of particle counts, size distribution and infectivity. J Virol Methods 144(1–2):122–132.

Wiedensohler A. 1988. An approximation of the bipolar charge-distribution for particles in the sub-micron size range. J Aerosol Sci 19(3):387–389.

Wyatt PJ. 1993. Light scattering and the absolute characterization of macromolecules. Anal Chim Acta 272(1):1–40.

Yamada T, Iwasaki Y, Tada H, Iwabuki H, Chuah MKL, VandenDriessche T, Fukuda H, Kondo A, Ueda M, Seno M, et al. 2003. Nanoparticles for the delivery of genes and drugs to human hepatocytes. Nature Biotechnol 21(8):885–890.

Zimm BH. 1948. The scattering of light and the radial distribution function of high polymer solutions. J Chem Phys 16(12):1093–1099.

Zolotukhin S, Byrne BJ, Mason E, Zolotukhin I, Potter M, Chesnut K, Summerford C, Samulski RJ, Muzyczka N. 1999. Recombinant adeno-associated virus purification using novel methods improves infectious titer and yield. Gene Ther 6(6):973–985.